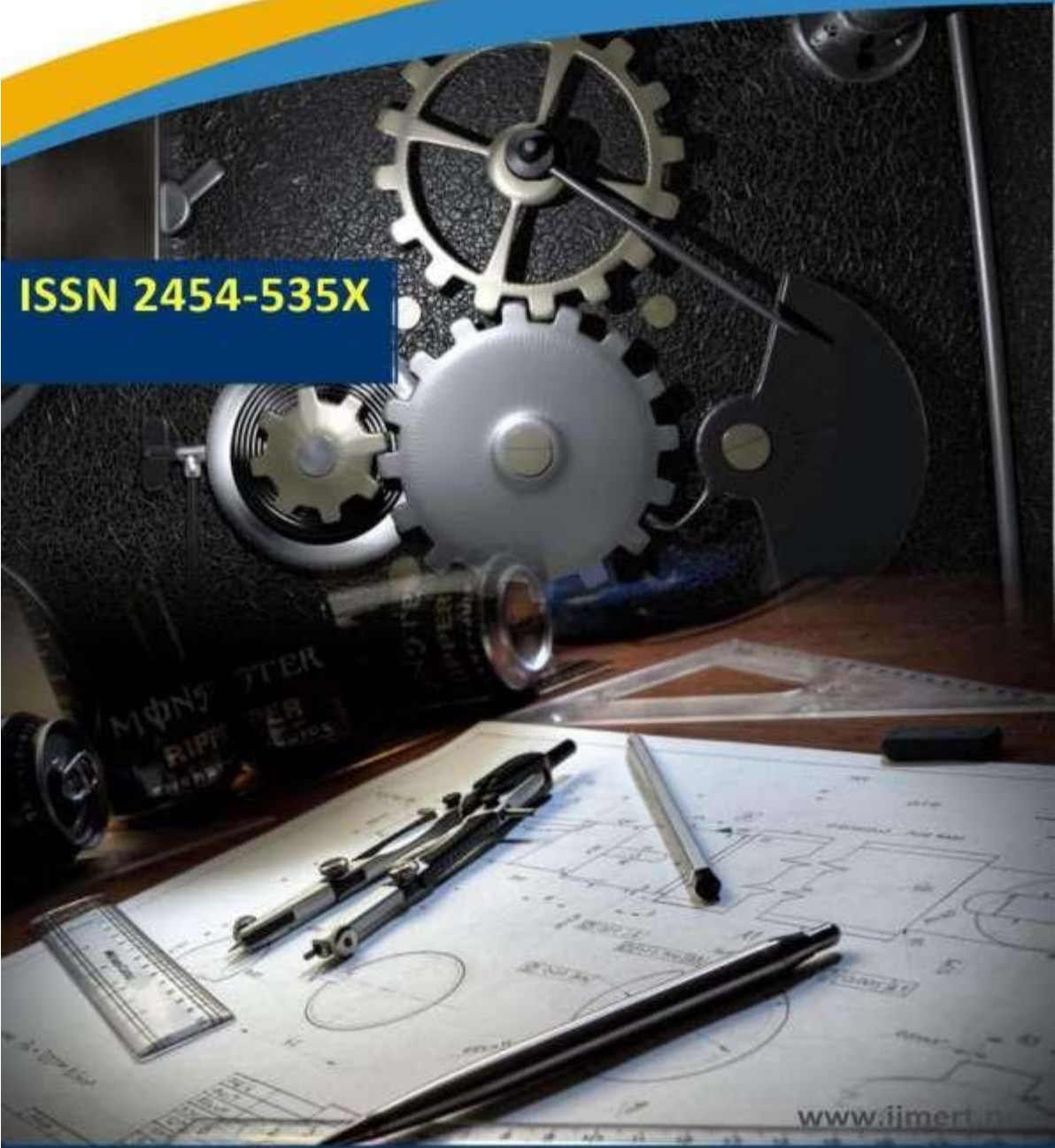




**International Journal of**  
Mechanical Engineering Research and Technology

**ISSN 2454-535X**



[www.ijmert.in](http://www.ijmert.in)

**Email ID: [info.ijmert@gmail.com](mailto:info.ijmert@gmail.com) or [editor@ijmert.net](mailto:editor@ijmert.net)**



# Assessing the steadiness and dependability of a GIS-integrated broadband current array sensing system

Anem Apparao, Koyyana Praveen, Padapana Usha Rani, Baratam Murali

---

## ABSTRACT

By keeping an eye on things like power frequency overvoltage, relative dielectric loss, and partial discharge, a broadband current array sensing system may help gas insulated switchgear identify defects even more accurately and prevent equipment problems. While designing a defect observer and calculating the system stability criteria under  $\infty$  conditions, the dynamic model of the system is examined and used to derive the system state equation. Using cloud models, we confirm the system's stability under varying packet loss rates and propose a strategy based on electromagnetic compatibility to keep packet loss rates below 50%.

---

**Keywords:** gas insulated switchgear, current sensing, stability, reliability, system control

---

## Introduction

Online monitoring and sensing dependability is in high demand due to the rising reliability requirements for gas insulated switchgear (GIS) [1]. It is difficult to immediately reflect the severe condition of internal flaws in the equipment using traditional partial discharge (PD) sensing technologies like ultra-high frequency and ultrasound since they are independent and indirect measures. The inability to integrate systems is a result of the absence of a common sensing

infrastructure [2-4]. The Broadband Current Array Sensing System (BCASS) measures the current at various frequencies of the equipment's location, allowing for live monitoring of crucial conditions like power loss and power factor (PF) while the equipment is operating. Sensor data communication, analysis result transmission, and sensor measurement feedback management are all handled by BCASS via wired and wireless means [5-7]. Substation environments are common places to find wireless sensor networks,

---

**Associate Professor<sup>1</sup>, Assistant Professor<sup>2,3,4</sup>**  
Sri Venkateswara College of Engineering & Technology,  
Etcherla, Srikakulam, Andhra Pradesh-532410  
Department of Electrical and Electronics Engineering

---

one of its key components is routing. If data is not collected promptly and accurately, routing performance will suffer. The quality of routing work is likely to decline with unexpected changes in substation circumstances and changes in sensor array architecture since wireless sensor networks are restricted by communication capabilities, number of nodes, node power consumption, and operating modes. Array sensing systems (networks) rely on routing algorithms that can withstand changes in topology and operating circumstances while still providing reliable functionality. Conventional reasoning It is difficult to precisely define the notion of stability in sensor network routing when substation conditions and control laws are intricate because stability judgments are restricted to a narrow range,

do not include analytical solutions, and lack clear boundary conditions [8–10]. Thus, in order to assess the reliability of sensor network routing, the idea of a cloud model is used. This article sets up the dynamic model of the present array sensing technology that is utilized for online GIS monitoring. Currents such as iron core grounding current, bushing end screen current, high-frequency PD, and big overvoltage current are among those that are monitored. In order to support the design of BCASS for GIS devices, a stable control system is developed for adaptive fault observers of uncertain linear time invariant (LTI) systems. This system is then used to suggest the cloud mode and quantify the stability of various routing algorithms.

**1 Stability of BCASS applied to GIS**

1.1 Sensor layout and current types

2 Input, sensor response, data transfer, AD conversion, and feature extraction make up the system dynamic model of a broadband current sensor array for GIS equipment. The variables that are taken into account are the following: GIS CT CB in-phase current, GIS CB grounding copper high frequency partial discharge current, GIS CB grounding copper big over-voltage current, and GIS CB grounding copper large power frequency current.

3 GIS CT-CB in-phase current, busbar large power frequency current (L-GCB-PT), busbar high frequency partial discharge current (pd-GCB-PT), and GIS-CT grounding copper

4 significant current at high power frequencies  $i_{L-GPT}$ . In Fig. 1, we can see the precise locations and arrays of different current sensors.

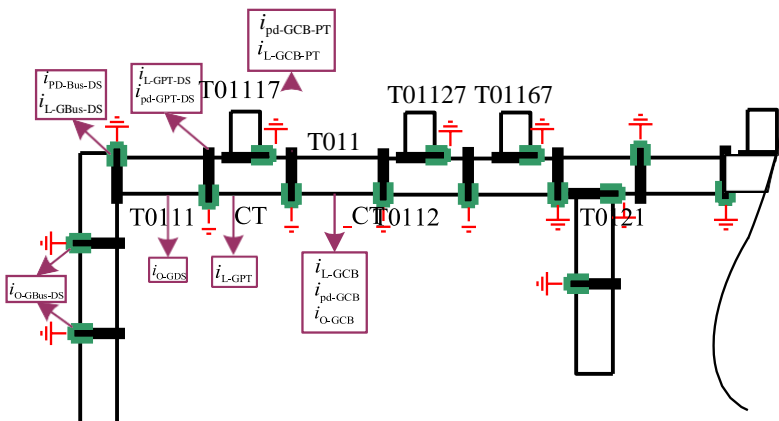


**Fig. 1.** Sensor layout and corresponding current types of BCASS

4.1 Dynamic model

The BCASS interpretation model for GIS includes  $H_{L-I} H_{L-AD}^T$  system is designed. Firstly, an improved Adaptive Fault

$$F_{Bus}(f_i, A_i, \varphi_i) \dot{y}_{GBus}$$

Estimation Algorithm (AFEA) is proposed, which utilizes stability theory and generalized inverse

matrix

ere,  $\dot{y}_{GCB}, \dot{y}_{GDS}$  and  $\dot{y}_{GBus}$  are the status of circuitbreakers, isolating switches, and busbar respectively. theory to enhance the algorithm's speed and accuracy. An analysis of the convergence interval and convergence rate is introduced to determine the unknown parameters

$$\begin{matrix} H_{L-1} & H_{L-AD} & 1 \\ H_{H-1} & H_{H-AD} & \end{matrix}$$

For a given circular area  $(\lambda, r)$  and scalar  $\gamma > 0, \sigma > 0$ , if the symmetric positive definite matrix

$P \in R^{n \times n}$  and symmetric matrix  $R_1 \in R^{r \times r}$  make the following equation hold true, IAFO can distribute the eigenvalue of  $(A - LC)$  within the unit circle  $D(\lambda, r)$ ,

When a time-varying fault occurs in the system, the first-order derivative of the fault with respect to time

$f(t)$  exists and the norm of  $f(t)$ ,  $f(t)$  is bounded, namely the existence of positive real numbers  $f_0, f_1$  makes  $\|f(t)\|_2 \leq f_0, \|\dot{f}(t)\|_2 \leq f_1$  valid. Therefore, the stability criterion can be derived as follows. and meet performance indicators  $H_\infty(\|\tilde{e}(t)\|_2 < \gamma \|\tilde{N}(t)\|_2)$ , the Gain Matrix of IAFO can be set as  $L = P^{-1}Y$ .

Feed back of over voltage

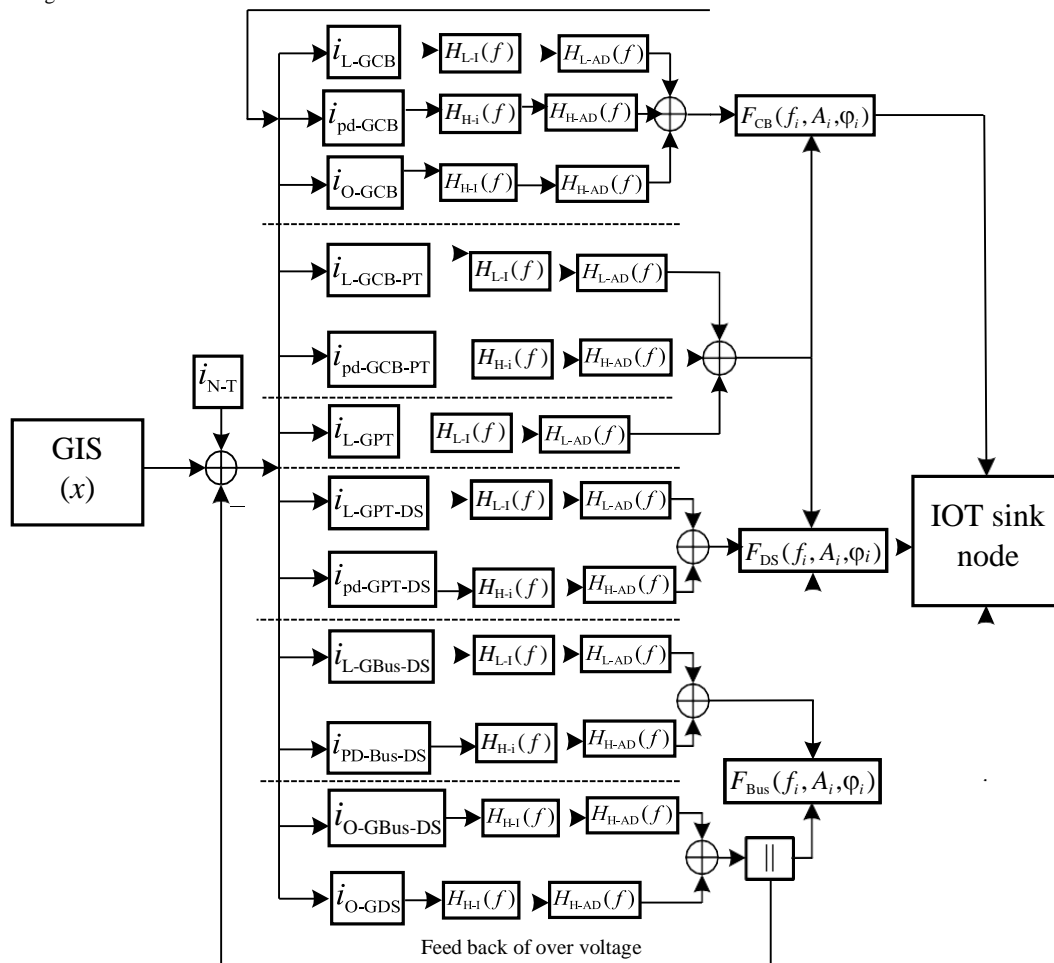


Fig. 2. Sensor layout and corresponding current types of BCASS

IAFO ensures that  $((t), e_f(t))$  converges to the interval at a rate greater than  $e^{-at}$ . To further calculate stability criteria, the Lyapunov function is introduced as follows.



$$\begin{cases} V \leq \lambda_{\max}(P) \|e_x(t)\|_2 + \frac{1}{\sigma} \|e_f(t)\|_2 \leq \max\left[\lambda_{\max}(P), \frac{1}{\sigma}\right] (\|e_x\|_2 + \frac{1}{\sigma} \|e_f\|_2) \\ \dot{V}(t) \leq -\alpha V(t) + \varepsilon \end{cases}$$

If  $((t), e_f(t)) \in S$  and  $V \leq 0$ , the trajectory of  $(e_x(t), e_f(t))$  in outside is continuously approaching the set  $S$ . When  $\sigma > \frac{1}{\lambda_{\max}}$ , the stability condition of BCASS is shown in equation (7).

$$\alpha = \frac{\min(b_1, b_2)}{\lambda_{\max}}$$

An arbitrary relaxation system is defined as bounded input-bounded output stable. For LTI systems, the necessary and enough conditions for the stability can be defined as equation (8)

$0.949 \pm 0.033i, 0.964 \pm 0.050i, 0.986 \pm 0.061i$ . All poles are

within the unit circle, namely, the convergence domain of the system contains the unit circle, which indicates that the system is stable.

$$\sum_{n=-\infty}^{\infty} |h(n)| < \infty$$

### 5 Reliability of BCASS applied to GIS

5.1 Routing stability indicators For causal system transfer function  $h(n)$ , the Z- transform is defined as equation (9)

$$H(z) = \sum_{n=-\infty}^{+\infty} h(n)z^{-n} \tag{9}$$

Therefore, when the unit circle ( $|z|=1$ ) is contained in the convergence domain of  $H(z)$ , the LTI system is stable. The pole-zero plot of broadband current sensing array system are calculated, as shown in Fig. 3.

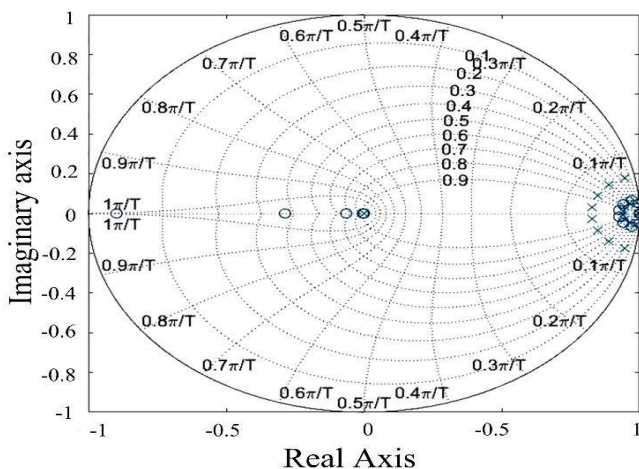


Fig. 3. Pole-zero plot of broadband current sensing array system

$0.941 \pm 0.177i$ , From the perspective of BCASS operation, considering node packet loss rate, number of sensors installed on nodes, unstable factors or faults during data packet transmission can lead to abnormal array sensor output results. Therefore, the routing stability of wireless sensor networks mainly includes three aspects: network conditions, average energy consumption, and network communication success rate.

The system transfer function consists of 9 pairs of conjugate poles:  $0 \pm 0i, 0.831 \pm 0.031i, 0.850 \pm 0.089i, 0.890 \pm 0.141i, 0.940 \pm 0.012i,$

The network conditions  $N_C$  including disturbances in the network environment and calculation methods during stability analysis, such as node loss rate and



node failure. The average energy consumption  $E_{dave}$  includes the total energy consumed by each sample node to transmit one data packet to its superior/subordinate nodes. The success rate of network communication  $S_r$  is defined as the ratio of the total number of data packets received by the upper/lower nodes to the total number of data packets sent by the same source nodes when the sample node sends a set of data packets to the upper/lower nodes as the source node.

For data centric wireless sensor networks, the reliability and immediacy of data transmission are the core issues in engineering, and the routing algorithm of wireless sensor networks plays a crucial role in data transmission. One of the concerns for electromagnetic interference or temporary disconnection of communication nodes).

C2 level, with good reliability, indicating moderate anti-interference ability. For example, the array sensing performance temporarily decreases under electro-magnetic interference, requiring short-term manual maintenance.

C3 level, reliable, indicating low immunity, such as reduced performance under electromagnetic interference, requiring long-term or short-term manual maintenance, resulting in reduced performance.

C4 level, poor reliability, indicating no immunity, such as direct damage to equipment under electromagnetic interference.

Reliability evaluation is divided into qualitative evaluation and quantitative evaluation according to cloud models. Qualitative evaluation is the mapping from stability space to stability space, while quantitative evaluation is the mapping from stability space to stability space. The 4-level reliability mapping relationship is defined as follows:

$$C_1 \Rightarrow c \in (0.8, 1]$$

operators is whether the routing algorithm can maintain stability in the event of external environmental changes and self-disturbances. Therefore, the focus of this project's research on routing stability is on the stability of routing data transmission, which mainly examines key factors that affect communication success rate, such as packet loss rate, the delay of base station receiving data packets, and the number of data packets. The routing stability is defined into four levels through language variables:

C1 level, with excellent reliability, indicating that the array sensing system can automatically recover to normal in the event of significant disturbances (such as

### 5.2 Routing stability inference rules based on two-dimensional cloud model

In the case of high packet loss rate in routing algorithms, if the array sensor network can still maintain a high success rate, it is obvious that the reliability of the array sensor network is C1, which means that routing stability cannot be measured solely from packet loss rate or a certain dimension. The routing stability inference rules of two-dimensional cloud model are represented as in Eqn. (11).

$$r_{ij}: (x_1 = A_i \& x_2 = B_j) \rightarrow y = C_k \tag{1}$$

1)

Here,  $r_{ij}$ ,  $x_1$ ,  $x_2$ ,  $y$  represent the inference rules, input and output respectively,  $A_i$  and  $B_j$  are the input rule prerequisites for cloud models,  $C_k$  is the result.  $x_1$  and  $x_2$  are Input to cloud generator  $P_{A_i, B_j}$  and the corresponding membership degree  $\mu_{ij, P}$  is obtained. The max membership degree  $\mu_{max}$  is calculated by rule selector, and the corresponding reliability level. The flow chart of

### 5.3 Reliability verification

To verify the reliability of BCASS in unicast routing, multicast routing, and tree routing networking scenarios, different node packet loss rates, communication success rate tests are conducted on three routing method. Each routing method is tested 10 times for each packet loss rate, with a nodes' packet loss rate of 50% as an example. The results are shown in Table 1.

**Table 1.** The network communication success rates

Method	#1	#2	#3	#4	#5	#6	#7	#8	#9	#10
Unicast routing	0.016	0.097	0.086	0.049	0.080	0.014	0.042	0.092	0.079	0.086



Multicast routing	0.166	0.104	0.095	0.093	0.068	0.076	0.074	0.039	0.066	0.007
Tree routing	0.471	0.403	0.338	0.365	0.360	0.462	0.359	0.232	0.395	0.313

According to section 3.2, reliability of each kind of routing with different packet loss rate is calculated, as shown in Table 2.

**Table 2.** The network communication success rates

Method	Parameter	Node's			Packet	
		10%	20%	30%	40%	50%
Unicast routing	success rate of communication	0.47	0.26	0.17	0.08	0.06
	Reliability level/Membership degree	$C_{41}/0.32$	$C_{42}/0.14$	$C_4/0.25$	$C_4/0.56$	$C_4/0.37$
	Reliability	0.30	0.05	0.10	0.26	0.28
Multicast routing	success rate of communication	0.60	0.33	0.21	0.10	0.08
	Reliability level/Membership degree	$C_3/0.82$	$C_{32}/0.48$	$C_4/0.12$	$C_4/0.46$	$C_4/0.35$
	Reliability	0.48	0.41	0.15	0.28	0.29
Tree routing	success rate of communication	0.93	0.81	0.72	0.47	0.34
	Reliability level/Membership degree	$C_{12}/0.51$	$C_{12}/0.85$	$C_{11}/0.31$	$C_{31}/0.23$	$C_{31}/0.20$
	Reliability	0.81	0.83	0.95	0.60	0.49

According to Table 2, when the packet loss rate is less than 50%, tree routing can achieve a higher network communication success rate. Further calculation of 2-D cloud model formed by the accuracy of the tree routing and p

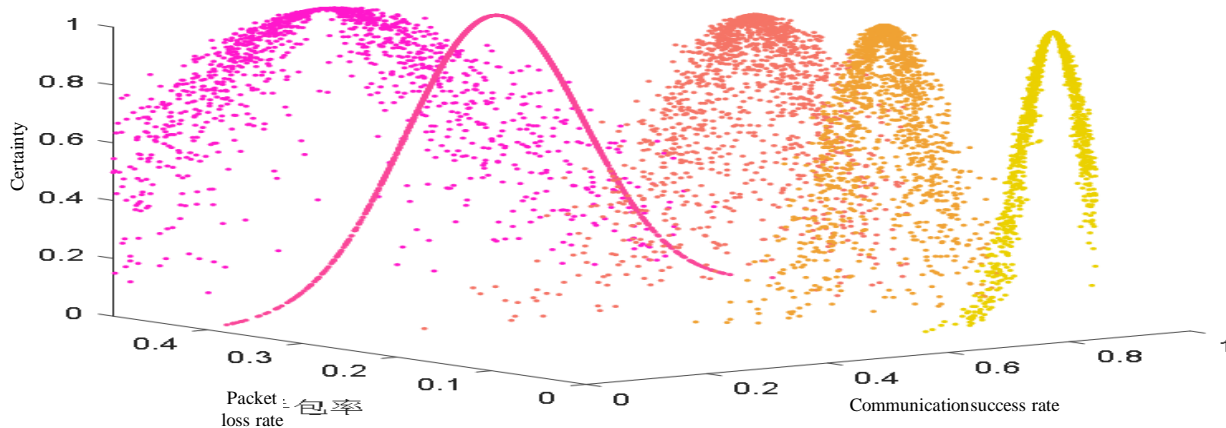


**Fig. 5.** 2-D cloud model of tree routing's reliability

6 The 2-D cloud model of tree routing states that for a given packet loss rate, the communication success rate and uncertainty both tend to follow a normal distribution, suggesting that the process is stochastic at rest. Measurements of communication reliability and believability are enhanced for a packet loss rate of 0.1, as the cloud space with a certainty level of 0.5 has a width of around 0.15 and a thickness of about 0.01. The evaluation results show a wide range of levels, the test results are more reliable, the entropy value is larger, and the cloud droplet thickness reaches its minimum value at 0.4 packet loss rate, but the width is larger than at 0.1-0.3 packet loss rate. This suggests that the super entropy of the communication success rate is lower. In order to keep the packet loss rate from reaching 50% during on-site application, it is recommended to include electromagnetic shielding measures into the routing and communication hardware and reduce the communication distance.

### Conclusion

7 To keep tabs on GIS currents, we suggest a BCASS design approach. A fault observer is designed to determine the system stability criteria, and the state equation is provided using the BCASS system dynamics model. Because of the observer's state feedback fault-tolerant controller, BCASS is very stable and converges quickly. To ensure the system's stability in

design, we use the  $b_{\infty}$  stability condition to determine nine sets of system poles, all of which fall within the unit circle. Using packet loss rate and communication success rate as examples, a reliability testing technique based on cloud model theory is created to perform reliability testing of BCASS in practical engineering. Various node packet loss rates are used to verify the reliability of unicast, multicast, and tree routing. Based on the findings, tree routing and electromagnetic compatibility prevention measures should be used if the packet loss rate is less than 50%.

### References

- [1] "RF PD signal propagation in GIS: Comparing S-parameter measurements with an RF transmission model for a short section of GIS," published in June 2016 by IEEE Transactions on Dielectrics and Electrical Insulation, is authored by G. Behrmann and J. Smajic. [2] "In-situ insulation test of 400 kV GIS," published in October 2008 by IEEE Transactions on Dielectrics and Electrical Insulation, article by H. Mohseni, J. Jadidian, A. A. Shayegani-akmal, E. Hashemi, A. Naieny, and E. Agheb. [3] "Insulation characteristics of GIS bus with conductive protrusion attached to the high-voltage electrode under lightning impulses with different wavefront times," published in the December 2019 issue of the IEEE Transactions on





Dielectrics and Electrical Insulation, has been authored by T. Wen, Y. Zhao, X. Fan, Q. Zhang, N. Shimomura, and W. Chen. [4] In the December 2011 issue of the IEEE Transactions on Dielectrics and Electrical Insulation, the authors T. Ito, M. Kamei, G. Ueta, and S. Okabe discuss "Improving the sensitivity verification method of the UHF PD detection technique for GIS," which is volume 18, issue 6, pages 1847–1853. [4] "Adaptive Tracking Control of A Class of First-Order Systems With Binary-Valued Observations and Time-Varying Thresholds," published in the 2011 December issue of the IEEE Transactions on Automatic Control, was written by J. Guo, J. -F. Zhang, and Y. Zhao. [6] In the January 2011 issue of the IEEE Transactions on Automatic Control, with the title "Supervisory Control of Uncertain Linear Time-Varying Systems," L. Vu and D. Liberzon wrote the article. "Event- Triggered Optimal Parallel Tracking Control for Discrete-Time Nonlinear Systems," published in June 2022 by IEEE

Transactions on Systems, Man, and Cybernetics: Systems, was written by J. Lu, Q. Wei, Y. Liu, T. Zhou, and F. -Y. Wang. In their article "Adaptive Fuzzy Decentralized Tracking Control for Large-Scale Interconnected Nonlinear Networked Control Systems," published in the October 2021 issue of the IEEE Transactions on Fuzzy Systems, the authors Ma, Wang, Qiu, and Karimi discuss adaptive fuzzy decentralized tracking control. [9] In the March–April 2018 issue of the IEEE Transactions on Services Computing, the authors L. Sun, J. Ma, H. Wang, Y. Zhang, and J. Yong present "Cloud Service Description Model: An Extension of USDL for Cloud Services," which can be found on pages 354–368, volume 11, issue 2. R. Garg, "MCDM-Based Parametric Selection of Cloud Deployment Models for an Academic Organization," in IEEE Transactions on Cloud Computing, vol. 10, no. 2, pp. 863-871, 1 April-June 2022, is cited as a source.